Transactions of the Korean Nuclear Society Spring Meeting
Jeju, Korea, May 12-13, 2016

Electrostatic Analysis of Annular Holes Penetrated by Shorted-Cable

Jaeyul Choo*, Hyung Tae Kim, Hyun Shin Park, and Youngsik Cho
Korea Institute of Nuclear Safety, 62 Gwahak-ro, Yuseong-gu, Daejeon, Korea
**Corresponding author: k728cjy@kins.re.kr*

1. Introduction

Cabinets have been generally used to install digital modules for instrumentation and control (I&C) in nuclear power plants. The cabinet includes lots of signal and power cables whose layout complies with regulatory guides [1]. The cabinet has an important role to protect the contained cables and digital modules for the safety function from the external electromagnetic (EM) source. Thus the immunity of an open cabinet against electromagnetic interference (EMI) numerically has been investigated using mode-matching method in [2].

Another path for the external EM source to impinge on inner cables and digital modules is the bottom hole of the cabinet that is penetrated by various cables. Especially the EMI can detrimentally influence on the digital modules through annular space caused by sealing the bottom hole of the cabinet incompletely. Thus it is recently required that the electromagnetic interpretation in the annular hole is performed to remedy electromagnetic problems. Using mode-matching method in conjunction with Weber and Hankel transforms, we evaluate the electric field and capacitance that are formed in the infinite space between top and bottom ground planes and annular holes penetrated by a shorted-cable.

2. Mode-Matching Formulation

2.1 Potential Representation

Fig. 1 illustrates the analyzed structure that is composed of top and bottom ground layers (thickness d_1 and d_2), a free-space layer (thickness h and dielectric constant ε_r), and a central shorted-cable (radius a) penetrating two holes of radii r_1 and r_2. The penetrating shorted-cable is at a potential V_0 whereas the two ground layers are at a potential of zero. The structure is divided into regions 1 through 5. In the following potential expressions, the right superscript denotes the corresponding region. The potentials Φ^1 and Φ^5 in region 1 and region 5 are expressed as (1) and (2) in the forms of Hankel transform. Based on the superposition principle and the Weber transform, the potentials in regions 2 and 3 are written as (3) and (4).

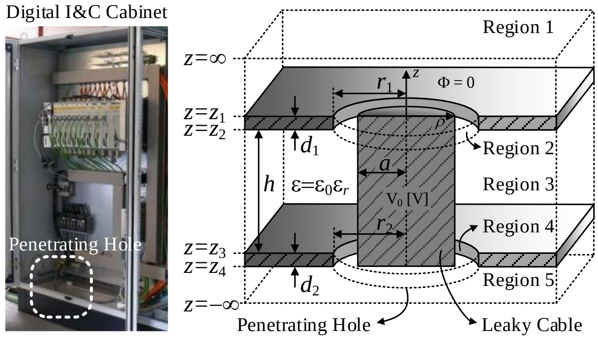

(a) (b)

Fig. 1. (a) Digital I&C cabinet with a penetrating hole, (b) Cross section of a hole penetrated by a shorted-cable.

$$\Phi^1 = \int_0^\infty \Phi_1(\zeta) e^{-\zeta z} J_0(\zeta\rho)\zeta\, d\zeta \tag{1}$$

$$\Phi^5 = \int_0^\infty \Phi_4(\zeta) e^{\zeta z} J_0(\zeta\rho)\zeta\, d\zeta \tag{2}$$

$$\Phi^2 = \frac{\ln\rho / r_1}{\ln a / r_1} V_0 + \sum_{m=1}^{\infty}\left(A_m e^{-k_{1m}z} + B_m e^{k_{1m}z}\right) R_0(k_{1m}\rho) a \tag{3}$$

$$\begin{aligned}\Phi^3 = & -\sum_{n=odd}^{\infty} \frac{4V_0 K_0(u_n\rho)}{n\pi K_0(u_n a)} \sin(u_n(z-z_2)) \\ & + \int_0^\infty \frac{\left[\Phi_2(\zeta)e^{-\zeta z} + \Phi_3(\zeta)e^{\zeta z}\right] Z_0(\zeta\rho)}{\left[J_0(\zeta a)\right]^2 + \left[N_0(\zeta a)\right]^2}\zeta\, d\zeta\end{aligned} \tag{4}$$

$$\Phi^4 = \frac{\ln\rho / r_2}{\ln a / r_2} V_0 + \sum_{m=1}^{\infty}\left(C_m e^{-k_{2m}z} + D_m e^{k_{2m}z}\right) R_0(k_{2m}\rho) \tag{5}$$

where

$$R_0(k_{Gm}\rho) = J_0(k_{Gm}\rho) - \frac{J_0(k_{Gm}a)}{N_0(k_{Gm}a)} N_0(k_{Gm}\rho) \tag{6}$$

$$Z_0(\zeta\rho) = J_0(\zeta\rho)N_0(\zeta\rho) - N_0(\zeta\rho)J_0(\zeta\rho) \tag{7}$$

Herein $J_0(\cdot)$ and $N_0(\cdot)$ are the Bessel functions of the first and second kinds of order 0, $K_0(\cdot)$ is the modified Bessel function of the second kind of order 0, the parameters k_{Gm} (G = 1, 2 and m = 1, 2, 3, ⋯) are the roots of $R_0(k_{Gm}r_G) = 0$, and $u_n = n\pi/h$ (n = 1, 3, 5, ⋯), respectively.

2.2 Enforcement of Boundary Conditions

In order to determine the unknown coefficients A_m, B_m, C_m, D_m, $\Phi_1(\zeta), \Phi_2(\zeta), \Phi_3(\zeta)$, and $\Phi_4(\zeta)$, four Dirichlet and four Neumann boundary conditions are required. The Dirichlet boundary conditions on the potential continuity and the Neumann boundary conditions on the normal derivative continuity at $z = z_1$ and $z = z_2$ are

$$\Phi^1\Big|_{z=z_1} = \begin{cases} V_0 & , \ 0<\rho<a \\ \Phi^2\Big|_{z=z_1} & , \ a<\rho<r_1 \\ 0 & , \ r_1<\rho<\infty \end{cases} \tag{8}$$

$$\Phi^3\Big|_{z=z_2} = \begin{cases} \Phi^2\Big|_{z=z_2} & , \ a<\rho<r_1 \\ 0 & , \ r_1<\rho<\infty \end{cases} \tag{9}$$

$$\left.\frac{\partial \Phi^1(\rho,z)}{\partial z}\right|_{z=z_1} = \left.\frac{\partial \Phi^2(\rho,z)}{\partial z}\right|_{z=z_1} \quad , \ a<\rho<r_1 \tag{10}$$

$$\left.\frac{\partial \Phi^2(\rho,z)}{\partial z}\right|_{z=z_2} = \varepsilon_r \left.\frac{\partial \Phi^3(\rho,z)}{\partial z}\right|_{z=z_2} \quad , \ a<\rho<r_1 \tag{11}$$

The other Dirichlet and Neumann boundary conditions at $z = z_3$ and $z = z_4$ can be similarly rewritten. Next applying the inverse Hankel and Weber transforms to Dirichlet and Neumann boundary conditions yields a set of simultaneous equations for the modal coefficients A_m, B_m, C_m, and D_m. It is possible to evaluate the A_m, B_m, C_m, and D_m after truncating the infinite series in the simultaneous equations.

3. Computed Results

The capacitance generally indicates how much the penetrating shorted-cable influences on adjacent objects. Based on Gauss's law the capacitance is calculated by

$$C = \frac{Q}{V_0} \tag{12}$$

where

$$Q = \oint_s \bar{D}\cdot d\bar{s} = \oint_s (-\varepsilon\nabla\bar{D})\cdot\hat{n}d\bar{s} = \oint_s p_s d\bar{s} \tag{13}$$

Herein P_s is surface charge density (C / m^2).

Using (12) and (13) we then calculated the capacitance between a penetrating shorted-cable and top and bottom ground layers when a = 0.2 m and a = 0.3 m in the condition of $d = 0.127a$, $h = 1.27a$, $r = 4a$, and $\varepsilon_r = 3.84$. To validate our analyzed results, we compared our computed capacitance with those by [3] as shown in Table I. Table I represents that the partial capacitance C_3 is dominant in electromagnetic coupling as well as our computed results has a favorable agreement with those of [3].

Table I: Calculated capacitance

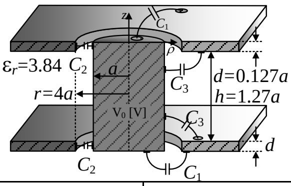		Zhang [3]	Ours
a = 0.2 m	C_1	-	18.3 fF
	C_2	3.9 fF	5.4 fF
	C_3	19.4 fF	17.6 fF
a = 0.3 m	C_1	-	27.5 fF
	C_2	5.5 fF	8.15 fF
	C_3	27.4 fF	29.1 fF

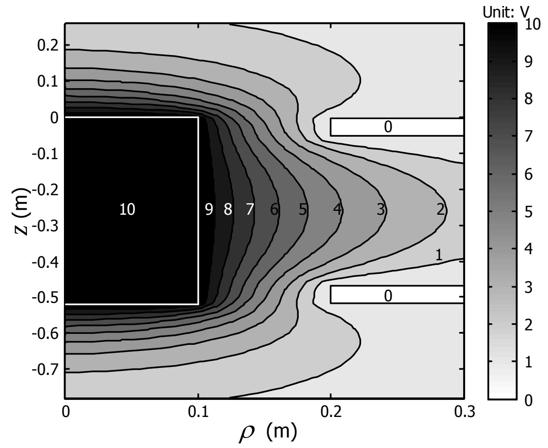

Fig. 2. Potential distribution when a = 0.1 m, $r_1 = r_2 = 2a$, $d_1 = d_2 = 0.6a$, and $h = 4a$.

We then calculated the potential distribution on the ρ–z plane as illustrated in Fig. 2 where the label number on the contour lines and the filled grey colors imply the strength of calculated potentials. The results in Fig. 2 shows that the potential distribution gradually changes from the central shorted-cable with 10 V to the outer ground layers with 0 V. The calculated capacitance and potential distribution provide us the insight to avoid EMI problem.

3. Conclusions

Based on the mode-matching method, we solved the electrostatic boundary-value problem for holes penetrating shorted-cable at the bottom of a digital I&C cabinet. The Weber transform and the Hankel transform were applied to formulate the electrostatic potential. The capacitance and potential distribution generated near the penetrating shorted-cable were computed and compared with the result from the previous study. The presented analysis provides the insight to avoid EMI problems at digital I&C cabinet in a nuclear power plant.

4. Acknowledgement

This work was supported by the Korea Institute of Nuclear Safety under the project 'Development of Proof

Test Model and Safety Evaluation Techniques for the Regulation of Digital I&C Systems used in NPPs' (no. 1305003−0315−SB130).

REFERENCES

[1] IEEE Standard Criteria for Independence of Class 1E Equipment and Circuits, IEEE Standard 384-2008, Dec. 2008.
[2] J. Choo, C. Jeong, and J. Choo, Transverse Electric Scattering of Open Cabinet in Nuclear Power Plants, IEEE Antennas and Wireless Propagation Letters, to be published.
[3] Y. Zhang, J. Fan, G. Selli, M. Cocchini, and F. Paulis, Analytical Evaluation of Via-plate Capacitance for Multilayer Printed Circuit Boards and Packages," IEEE Transactions on Microwave Theory and Techniques, Vol. 56, No. 9, pp. 2118–2128, Sep. 2008.